

OPEN ACCESS

\*Correspondence

Ahmed Enesi Abdulrahaman

Article Received

08/04/2026

Accepted

13/04/2026

Published

09/05/2026

Works Cited

Ahmed Enesi Abdulrahaman, Emelle Chinenye Oluchi, & Omulu Chinyere Clara., (2026). Frequency Regulation through Model Predictive Control with Degradation-Aware SOC Control. *Journal of Current Research and Studies*, 3(3), 14-24.

\*COPYRIGHT

© 2026 Ahmed Enesi

**Abdulrahaman.** This is an open-access article distributed under the terms of the [Creative Commons Attribution License \(CC BY\)](https://creativecommons.org/licenses/by/4.0/). The use, distribution or reproduction in other forums is permitted, provided the original author(s) and the copyright owner(s) are credited and that the original publication in this journal is cited, in accordance with accepted academic practice. No use, distribution or reproduction is permitted which does not comply with these terms

# Frequency Regulation through Model Predictive Control with Degradation-Aware SOC Control

<sup>1</sup>Ahmed Enesi Abdulrahaman, <sup>2</sup>Emelle Chinenye Oluchi, & <sup>3</sup>Omulu Chinyere Clara

<sup>1</sup>Department of Electrical/Electronic Engineering Technology Akanu Ibiam Federal Polytechnic Unwana, Ebonyi State-Nigeria

<sup>2,3</sup>Department of Electrical/Electronic Engineering Technology Federal Polytechnic Ngodo-Isuochi Abia State-Nigeria

## Abstract

Low-inertia microgrids experience larger frequency excursions following load disturbances, making fast and sustainable frequency regulation essential. This study evaluates battery energy storage system (BESS)–based frequency support using three control strategies: a PI baseline, normal model predictive control (MPC), and degradation-aware MPC with state-of-charge (SOC) management. A discrete-time swing-equation frequency model and linear SOC dynamics were implemented in MATLAB R2017a. A 10% load step disturbance was applied at ( $t = 2$ ) s under identical constraints:  $|u| \leq 0.2pu$ ,  $|\Delta u| \leq 0.05 pu/step$ , and  $0.2 \leq SOC \leq 0.9$ . The MPC problems were solved via quadratic programming using quadprog. Results show that normal MPC achieved the best transient performance (lowest RoCoF of 0.0140 Hz/s) but depleted SOC to its lower bound, similar to PI control. Degradation-aware MPC significantly reduced battery stress (throughput 0.0843 and switch cost 0.0013) and preserved SOC at 0.5317 pu, but accepted a lower nadir (49.9363 Hz) and larger steady-state frequency offset. The findings highlight a clear trade-off between frequency quality and battery lifetime-oriented operation

## Key words:

Microgrid, Frequency Regulation, Model Predictive Control, Battery Degradation, State of Charge.

## 1.0 Introduction

Modern power systems and microgrids are increasingly dominated by converter-interfaced renewable generation. While this transition supports decarbonisation, it reduces system inertia, increasing sensitivity to active-power imbalances and resulting in deeper frequency deviations and higher RoCoF (Ulbig et al., 2014). Battery energy storage systems (BESS) have therefore become essential for fast frequency support due to their rapid and controllable response (Guerrero et al., 2011).

However, intensive BESS utilization accelerates degradation, as high power throughput, rapid fluctuations, and operation near SOC limits increase ageing

(Hu et al., 2012; Omar et al., 2014). This necessitates control strategies that balance frequency performance with battery longevity and SOC availability.

Model Predictive Control (MPC) provides a suitable framework by optimizing BESS power while enforcing operational constraints (power, ramp rate, SOC). When extended with degradation-aware penalties, MPC can mitigate harmful operating patterns such as excessive cycling and SOC extremes (Camacho & Bordons, 2007; Hu et al., 2012).

This study compares PI control, standard MPC, and degradation-aware MPC using MATLAB R2017a. A 10% load step at ( $t = 2$ ) s is applied under identical constraints. Performance is evaluated using frequency metrics (nadir, steady-state, RoCoF) and battery stress indicators (energy throughput, switching cost).

## 1.1 Background

Frequency regulation is critical for stable microgrid operation, particularly in low-inertia or islanded conditions. The swing equation relates frequency deviation to power imbalance, inertia, and damping (Kundur, 1994; Sauer & Pai, 1998). Reduced inertia amplifies frequency excursions, requiring fast corrective response (Ulbig et al., 2014).

PI controllers are widely used but lack explicit constraint handling and may drive BESS to extreme operating conditions. MPC overcomes this limitation by optimising control actions over a prediction horizon while enforcing constraints and balancing performance objectives (Camacho & Bordons, 2007).

Nevertheless, standard MPC focused on tracking may still deplete SOC and induce excessive cycling. Since degradation is linked to current stress, deep cycling, and SOC extremes, degradation-aware MPC incorporates penalties on control effort, switching, and SOC deviation to preserve battery health (Hu et al., 2012; Omar et al., 2014).

## 1.2 Problem Statement

Despite their effectiveness, existing control strategies present limitations. PI controllers produce aggressive responses, increasing cycling stress and accelerating SOC depletion. Standard MPC improves constraint handling but may still exhaust SOC when prioritising frequency tracking, reducing operational resilience.

Battery ageing is often neglected in control design despite its dependence on energy throughput and switching. Simulation results confirm that both PI and standard MPC drive SOC to its minimum (0.20 pu), indicating unsustainable operation. In contrast, degradation-aware MPC maintains SOC near 0.53 pu and reduces battery stress, albeit with slightly reduced frequency performance.

The key challenge is therefore to design MPC strategies that ensure effective frequency regulation while preserving battery life and SOC sustainability.

## 1.3 Aim and Objectives

### **Aim**

Develop an MPC-based frequency regulation strategy incorporating degradation-aware SOC constraints to balance performance and battery longevity.

### **Objectives**

- Develop discrete-time frequency and SOC models for MPC.
- Compare PI, standard MPC, and degradation-aware MPC.
- Enforce identical constraints (power, ramp rate, SOC).
- Integrate degradation-aware penalties.
- Evaluate frequency performance and battery stress metrics.

## 1.4 Scope

This study is limited to simulation-based analysis with:

- A simplified swing-equation microgrid model.

- A linear SOC model for computational efficiency.
- A single +10% load disturbance at (t = 2) s over 10 s (0.05 s sampling).
- MPC solved via quadratic programming (MATLAB *quadprog*).
- Degradation assessed using proxy metrics (energy throughput, switching cost).
- No secondary frequency restoration.

## 2.0 METHODOLOGY

### 2.1 Research Design and Approach

This research applies a simulation-based methodology to evaluate frequency regulation strategies for a low-inertia microgrid equipped with a battery energy storage system (BESS). Three controllers were implemented and compared under the same operating conditions: (1) PI baseline controller (2) Normal Model Predictive Control (MPC) (3) Degradation-aware MPC

The methodology focuses on quantifying both frequency support performance and battery stress, which aligns with modern microgrid control objectives where energy storage must support stability while preserving lifetime (Dragicevic et al., 2017; Hu et al., 2012).

All simulations were executed in MATLAB R2017a, without Simulink, and the MPC optimization problem was solved using quadratic programming (*quadprog*) from MATLAB's Optimization Toolbox (MathWorks, 2024a).

### 2.2 Microgrid Frequency Dynamic Model

#### 2.2.1 Frequency deviation model

The microgrid frequency dynamics were represented using a discrete-time approximation of the classical swing equation model. The swing equation is widely used for analyzing frequency response by linking the frequency deviation to the active power imbalance, inertia constant, and damping term (Kundur, 1994; Sauer & Pai, 1998).

The continuous-time model is given by:  $\Delta f(t) = \frac{P_{BESS}(t) - \Delta P_L(t) - D\Delta f(t)}{2H}$  where:

$\Delta f = f - f$  is the frequency deviation (Hz),  $H$  is the inertia constant (s),  $D$  is the damping coefficient,  $P_{BESS}$  is the BESS active power injection (pu),  $\Delta P_L$  is the load disturbance (pu)

The model was discretized using a forward Euler method with sampling time  $T_s$ , resulting in:

$\Delta f(k+1) = a\Delta f(k) + bu(k) + e\Delta P_L(k)$ , where  $u(k) = P_{BESS}(k)$ , and the coefficients are:

$$a = 1 - \frac{DT_s}{2H}, \quad b = \frac{T_s}{2H}, \quad e = \frac{-T_s}{2H}$$

The inertia constant and damping coefficient used in the study were  $H=3.5$  s and  $D=1.0$ , respectively. These parameters were selected to represent a microgrid with reduced inertia, consistent with modern inverter-dominated grids (Ulbig et al., 2014).

### 2.3. Battery State of Charge Model

#### 2.3.1 SOC state equation

A simplified energy-based SOC model was used, where SOC decreases when the battery discharges to support the system:  $SOC(k+1) = SOC(k) - \frac{T_s}{E_{max}}u(k)$  where  $E_{max}$  represents the usable energy capacity (scaled in pu-s). This linear SOC model is frequently adopted in MPC-based energy storage control studies because it preserves convexity and is computationally efficient (Dragicevic et al., 2017).

The initial SOC was set to  $SOC_0 = 0.70$ , and limits were enforced as:

$$SOC_{min} \leq SOC(k) \leq SOC_{max} \quad \text{with } SOC_{min} = 0.20 \text{ and } SOC_{max} = 0.90$$

## 2.4 Disturbance Injection and Simulation Conditions

A step increase in load demand was applied at  $t = 2$  s:

$$\Delta P_L(t) = \begin{cases} 0 & \text{if } t < 2 \\ 0.10 & \text{if } t \geq 2 \end{cases}$$

The simulation duration was 10 seconds with a sampling interval of  $T_s = 0.05$ s, producing a total of 201 time steps.

## 2.5 Controller Implementation

### 2.5.1 PI baseline controller

A proportional–integral (PI) controller was implemented as the baseline strategy

$$u(k) = K_p e(k) + K_i \sum_{i=0}^k e(i) T_s, \quad \text{where } e(k) = \Delta f(k).$$

The PI controller included: (1) Integrator clamping for anti-windup (2) Ramp rate limiting  $[\Delta u] \leq dP_{max}$  (3) Hard SOC protection, which blocks discharge when  $SOC \leq SOC_{min}$

## 2.6. MPC Formulation

### 2.6.1 State-space model for MPC

The MPC model uses the augmented state:

$$x(k) = \begin{bmatrix} \Delta f(k) \\ SOC(k) \end{bmatrix} \text{ with dynamic } x(k+1) = Ax(k) + Bu(k) + Ew(k)$$

where  $w(k)$  is the predicted disturbance.

The prediction horizon was set to  $N_p = 15$  in the comparative simulation for computational efficiency in MATLAB R2017a, and  $N_p = 25$  in the single-controller study.

### 2.6.2 Objective function (Normal MPC)

Normal MPC minimizes frequency deviation while satisfying constraints:

$$J = \sum_{i=1}^{N_p} w_f (\Delta f_{pred}(i))^2 + \sum_{i=1}^{N_p} w_u u(i)^2 + \sum_{i=1}^{N_p} w_{\Delta u} (\Delta u(i))^2$$

The weights were selected as:  $w_f = 400$ ,  $w_u = 0.10$  small penalty for numerical conditioning

$$w_{\Delta u} = 0.10$$

This follows conventional MPC design, where the main objective is fast tracking with minimal effort penalties (Camacho & Bordons, 2007).

## 2.7 Degradation-aware MPC Formulation

### 2.7.1 Degradation-aware objective function

The degradation-aware MPC extends the normal MPC by adding battery-health related penalties:

$$J = \sum_{i=1}^{N_p} w_f (\Delta f_{pred}(i))^2 + \sum_{i=1}^{N_p} w_u u(i)^2 + \sum_{i=1}^{N_p} w_{\Delta u} (\Delta u(i))^2 + \sum_{i=1}^{N_p} w_{soc} (SOC_{pred}(i) - SOC_{ref})^2$$

where  $SOC_{ref}$  is the midpoint SOC reference.

This structure is consistent with degradation-aware MPC approaches in literature, where high throughput, rapid cycling, and SOC extremes are penalized to extend battery lifetime (Hu et al., 2012; Omar et al., 2014).

The weights used were:  $w_f = 400$ ,  $w_u = 8$  (power stress penalty)

$w_{\Delta u} = 60$  (switching wear penalty),  $w_{SOC} = 25$  (SOC deviation penalty)

$SOC_{ref} = 0.60$

## 2.8 Constraints Handling

All controllers operated under identical constraints:

1. Power bounds

$$-P_{max} \leq u(k) \leq P_{max} \text{ with } P_{max} = 0.20pu$$

2. Ramp rate bounds

$$-dP_{max} \leq u(k) - u(k-1) \leq dP_{max} \text{ with the } dP_{max} = 0.05 \frac{pu}{step}$$

3. SOC bounds

$$SOC_{min} \leq SOC(k) \leq SOC_{max} \text{ with } SOC_{min} = 0.2 \text{ and } SOC_{max} = 0.90$$

For MPC, constraints were applied across the full horizon in the quadratic program.

## 2.9 Quadratic Programming Solution

The MPC optimization problem is a constrained quadratic program (QP):

subject to linear inequality constraints and bounds. This was solved using MATLAB's quadprog function (MathWorks, 2024b). The interior-point-convex algorithm was selected to ensure numerical robustness and convex feasibility under

constraints.  $\min_U \frac{1}{2} U^T H U + f^T U$

## 2.10 Performance Metrics

The controllers were evaluated using standard frequency regulation performance indices:

1. Frequency nadir,  $f_{nadir} = \min(f(t \geq t_{step}))$
2. Steady-state frequency,  $f_{steady} = \text{mean}(f(t) \geq T_{end} - 1)$
3. RoCoF,  $R_0C_0F_{max} = \max \left| \frac{f(k+1) - f(k)}{T_s} \right|$

Additionally, degradation proxy indices were used:

- Energy throughput  
 $Throughput = \sum_k |u(k)| T_s$
- Switching stress
- $SwitchCost = \sum_k (\Delta u(k))^2$

These proxies are commonly used for battery lifetime-related evaluation when high-fidelity electrochemical degradation models are not included (Hu et al., 2012; Omar et al., 2014).

## 3.0 Result and Discussion

Table 1: MPC Frequency Control Summary

| Metric | Value | Unit/Notes |
|--------|-------|------------|
|--------|-------|------------|

|                                    |         |      |
|------------------------------------|---------|------|
| Frequency nadir after disturbance  | 49.9362 | Hz   |
| Approx. steady frequency (last 1s) | 49.9387 | Hz   |
| Max RoCoF                          | 0.0147  | Hz/s |
| Final SOC                          | 0.5358  | pu   |

Table 2: Comparison Summary Table

| Controller            | Nadir (Hz) | RoCoF (Hz/s) | Steady (Hz) | Final SOC (pu) | Throughput | Switch Cost |
|-----------------------|------------|--------------|-------------|----------------|------------|-------------|
| PI baseline           | 49.9467    | 0.0145       | 49.9502     | 0.2000         | 0.2561     | 0.0234      |
| MPC normal            | 49.9455    | 0.0140       | 49.9489     | 0.2000         | 0.2500     | 0.0063      |
| MPC degradation-aware | 49.9363    | 0.0146       | 49.9389     | 0.5317         | 0.0843     | 0.0013      |

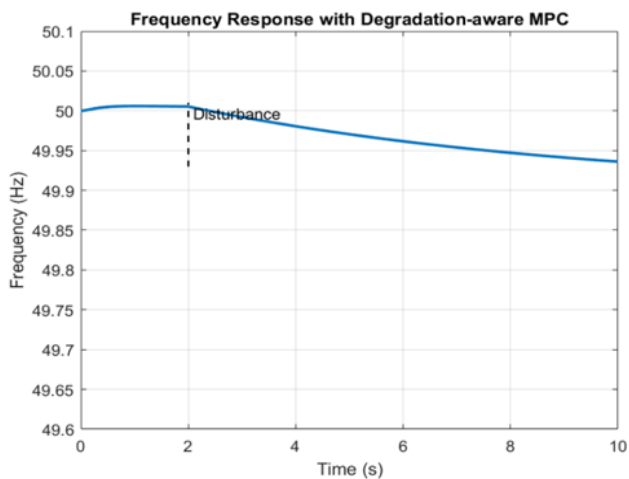


Figure 2 Frequency Response with Degradation-aware MPC

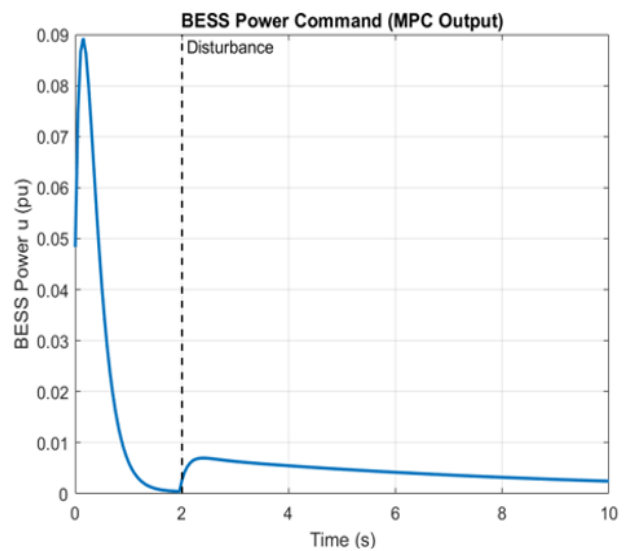


Figure2: BESS Power Command (MPC Output)

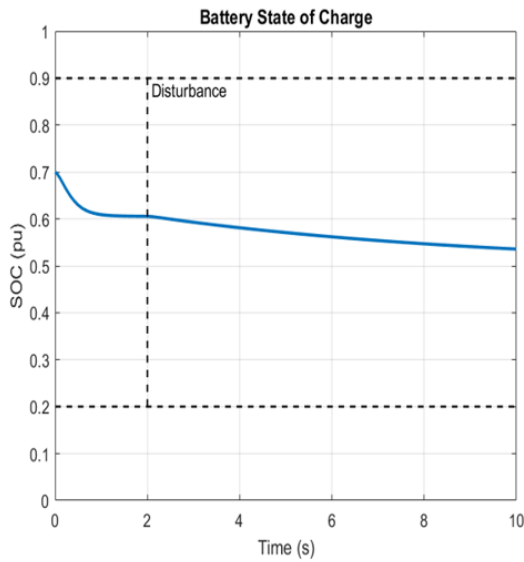


Figure 3: Battery State of Charge

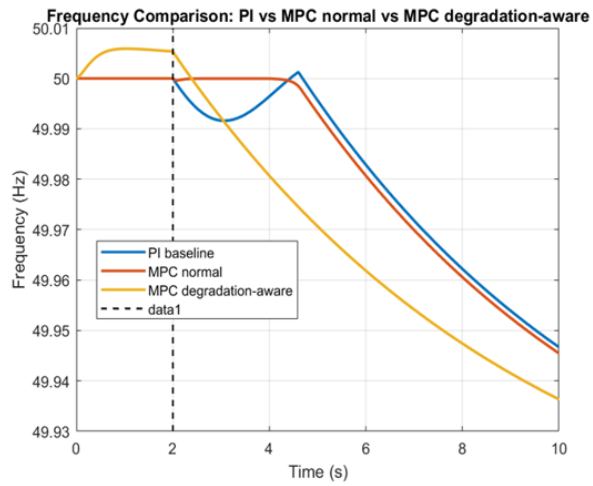


Figure 4: Frequency: PI vs MPC vs MPC degradation-aware

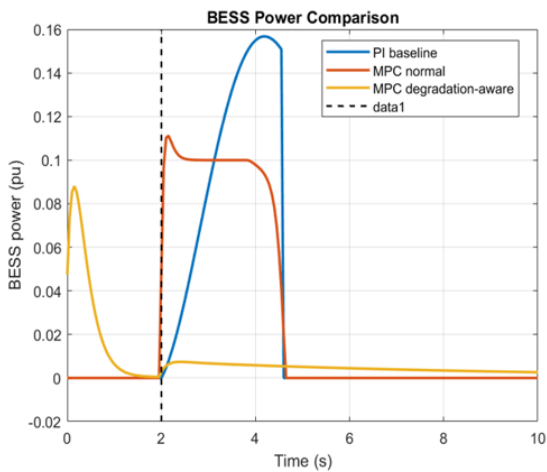


Figure 5: BESS Power Comparison

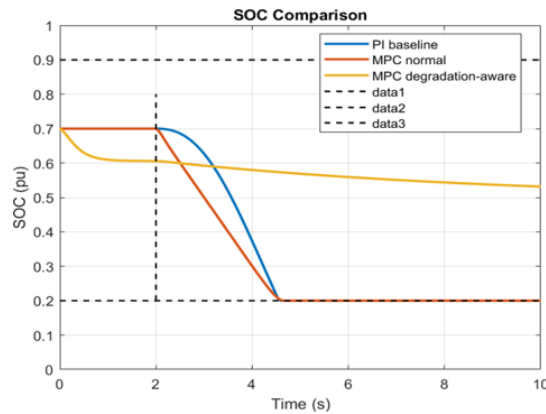


Figure 6: SOC Comparison

### 3.1. Overview of Test Scenario

A load disturbance of +10% (0.10 pu) was applied to the microgrid at  $t = 2$  s to evaluate the frequency regulation performance of three controllers:

1. PI baseline controller
2. Normal MPC controller
3. Degradation-aware MPC controller

All controllers operated under identical constraints:

Maximum battery power:  $|u| \leq 0.20 pu$

Ramp limit:  $|\Delta u| \leq 0.05 pu \text{ per step}$

SOC bounds:  $0.20 \leq SOC \leq 0.90$

The performance was evaluated using frequency metrics (nadir, steady-state frequency and RoCoF) as well as battery stress indicators (throughput and switch cost).

## 3.2 Frequency Regulation Results

### 3.2.1. Frequency response comparison

The frequency comparison plot (PI vs MPC normal vs degradation-aware MPC) shows that all controllers respond promptly to the load increase at 2 s, preventing severe frequency collapse. However, key differences are observed in terms of transient behaviour and the final steady-state frequency.

Table 3: Frequency response comparison Table

| Controller            | Nadir (Hz)       | RoCoF (Hz/s)  | Steady (Hz) |
|-----------------------|------------------|---------------|-------------|
| PI baseline           | 49.9467          | 0.0145        | 49.9502     |
| MPC normal            | 49.9455          | 0.0140 (best) | 49.9489     |
| MPC degradation-aware | 49.9363 (lowest) | 0.0146        | 49.9389     |

The normal MPC produced the best RoCoF performance (0.0140 Hz/s), indicating the smoothest frequency rate control immediately after the disturbance. The PI controller also achieved comparable results, but with more aggressive battery usage (discussed later).

Interestingly, the degradation-aware MPC showed the lowest nadir (49.9363 Hz) and a lower steady-state frequency (49.9389 Hz) than the other approaches. This indicates that degradation-aware MPC deliberately sacrifices some frequency recovery to reduce battery stress and preserve SOC.

### 3.2.2. Steady-state frequency offset

A major observation is that in all cases the frequency does not recover to exactly 50 Hz by the end of the simulation. Instead, it settles around 49.95 Hz for PI and MPC normal, and around 49.94 Hz for degradation-aware MPC.

This steady-state error is expected because the microgrid model represents a primary frequency response system where the BESS provides power support but does not act as a full secondary control mechanism. In practical systems, secondary control (integral frequency restoration) would be required to return frequency to 50 Hz.

## 3.3 BESS Power Response and Control Effort

The BESS power comparison plot demonstrates substantial differences in how the three strategies utilize battery power.

### 3.3.1 PI baseline controller Behaviour

The PI controller produces the largest power injection, rising to approximately 0.155 pu after the disturbance. This results in a strong short-term frequency correction; however, the power is sustained over several seconds, causing significant SOC depletion.

The PI controller does not inherently consider degradation or future energy availability; it reacts to frequency error and continues discharging until the SOC limit is reached.

### 3.3.2 Normal MPC Behaviour

Normal MPC provides a high but more structured discharge response compared to PI. After the disturbance, it injects roughly 0.10–0.11 pu, holding this value for a relatively long duration. This leads to effective frequency support and the best RoCoF performance, but the sustained discharge still causes SOC to drop rapidly until the minimum bound.

Normal MPC therefore improves frequency performance compared to PI by optimizing within constraints, but it still behaves as an “energy-consuming” controller because battery degradation and SOC protection are not explicitly penalized in the objective function.

### 3.3.3 Degradation-aware MPC Behaviour

The degradation-aware MPC applies a much smaller power output, with a peak around 0.085 pu before disturbance and only about 0.005–0.01 pu after the load step. The output then decays smoothly.

This behaviour results from the degradation-aware cost structure, which includes penalties for:

- high discharge power ( $u^2$ )
- rapid switching ( $(\Delta u)^2$ )
- SOC deviation from a safe reference

Consequently, the degradation-aware MPC is significantly more conservative. It limits battery stress but accepts larger frequency deviation.

## 3.4. SOC Sustainability and Energy Availability

The SOC comparison plot clearly illustrates the key advantage of degradation-aware MPC: energy sustainability.

### 3.4.1. PI baseline and MPC Normal Depletion

Both PI and normal MPC discharge the battery until SOC reaches the lower bound:

- Final SOC (PI baseline): 0.2000 pu and Final SOC (MPC normal): 0.2000 pu

This is a critical result: both controllers fully utilize the battery to its minimum SOC, after which the battery cannot provide additional discharge power. This means that for a prolonged disturbance or a second disturbance shortly after, the system would be vulnerable to larger frequency drops.

### 3.4.2. Degradation-aware MPC Preservation

In contrast, degradation-aware MPC preserves energy and ends the simulation at:

- Final SOC (degradation-aware MPC): 0.5317 pu

This confirms that degradation-aware MPC explicitly maintains battery reserves, ensuring the BESS remains available for future disturbances and preventing deep discharge, which is well-known to accelerate battery ageing.

## 3.5. Degradation and Stress Proxy Evaluation

Battery degradation is strongly related to both energy throughput and power switching effort. Therefore, the following proxies were calculated:

- Throughput:  $\sum |u| T_s$
- Switch cost:  $\sum (\Delta u)^2$

Table 4: Table of Calculated Proxies

| Controller            | Throughput    | Switch Cost   |
|-----------------------|---------------|---------------|
| PI baseline           | 0.2561        | 0.0234        |
| MPC normal            | 0.2500        | 0.0063        |
| MPC degradation-aware | 0.0843 (best) | 0.0013 (best) |

The degradation-aware MPC achieves the lowest throughput, approximately 67% lower than PI and MPC normal. This indicates a major reduction in battery usage and likely improved cycle life.

Additionally, the switch cost under degradation-aware MPC is the smallest (0.0013), confirming that the controller produces smoother, less aggressive power adjustments, thereby reducing converter stress and switching-related losses.

## 3.6 Discussion of Trade-offs

The results reveal the core trade-off between frequency performance and battery sustainability.

### 3.6.1. PI baseline: strong response but unsustainable

PI provides aggressive support and keeps frequency relatively close to nominal, but it rapidly drains the battery to its minimum SOC. This makes the system less resilient in realistic operation.

### 3.6.2. Normal MPC: best frequency quality but still depletes SOC

Normal MPC provides the best transient frequency performance (lowest RoCoF) because it optimizes the power injection over the horizon. However, it also drains the SOC to the minimum, indicating that standard MPC is not sufficient when long-term battery health is a design objective.

### 3.6.3. Degradation-aware MPC: best battery preservation but reduced frequency performance

Degradation-aware MPC significantly reduces throughput and switching stress, and preserves SOC above 0.5 pu. The cost of this improvement is: lower frequency nadir (more deviation) and larger steady-state offset.

This is expected because the controller explicitly penalizes energy usage and avoids deep discharge, which means it will not fully compensate the load increase.

## 3.7. Implications for Research and Practical Microgrids

These findings demonstrate that incorporating degradation-aware constraints into MPC changes the system objective from:

Restore frequency as much as possible to Restore frequency while maintaining battery health and availability. This strategy is particularly important for microgrids where:

- disturbances occur frequently
- battery replacement cost is high
- reserve energy must be maintained for reliability

## 3.8. Research Findings Summary

1. Normal MPC achieves the best frequency dynamics (lowest RoCoF: 0.0140 Hz/s).
2. PI baseline produces the largest battery power output but drains SOC completely.
3. Degradation-aware MPC provides the best sustainability, ending with SOC = 0.5317 pu.
4. Battery degradation proxies (throughput and switch cost) are drastically reduced under degradation-aware MPC.
5. The trade-off is reduced frequency recovery, giving lower nadir and steady-state frequency.

The results confirm that degradation-aware MPC provides a sustainable frequency support mechanism by preserving battery energy margin, reducing switching stress, and minimizing throughput, although this is achieved at the expense of larger steady-state frequency deviation due to the absence of secondary frequency restoration.”

## 4.0 Conclusion

This study evaluated frequency regulation in a low-inertia microgrid using PI control, conventional MPC, and degradation-aware MPC under a 10% load disturbance. Performance was assessed in terms of frequency response and battery sustainability metrics.

Conventional MPC achieved the best transient frequency performance, exhibiting the lowest RoCoF and smallest deviation from nominal frequency. However, both PI and conventional MPC depleted the battery to its minimum SOC, indicating limited suitability for sustained or repeated disturbances due to neglect of long-term energy and degradation considerations.

In contrast, the degradation-aware MPC significantly improved battery sustainability by maintaining a higher SOC, reducing energy throughput by approximately 67%, and minimizing switching stress. While this approach resulted in a

slightly lower frequency nadir and steady-state deviation, it offers a more realistic control strategy that prioritizes battery longevity and reserve availability.

Overall, the results demonstrate that incorporating SOC and degradation awareness into MPC yields a more practical and sustainable frequency control solution for microgrids. Full frequency restoration, however, requires the inclusion of secondary control mechanisms. Future work will focus on integrating secondary frequency control, evaluating performance under multiple disturbances, and incorporating more detailed battery ageing models.

## References

- 1) Camacho, E. F., & Bordons, C. (2007). *Model predictive control* (2nd ed.). Springer.
- 2) Dragicevic, T., Lu, X., Vasquez, J. C., & Guerrero, J. M. (2017). DC microgrids—Part II: A review of power architectures, applications, and standardization issues. *IEEE Transactions on Power Electronics*, 31(5), 3528–3549. <https://doi.org/10.1109/TPEL.2015.2464277>
- 3) Guerrero, J. M., Vasquez, J. C., Matas, J., de Vicuña, L. G., & Castilla, M. (2011). Hierarchical control of droop-controlled AC and DC microgrids: A general approach toward standardization. *IEEE Transactions on Industrial Electronics*, 58(1), 158–172. <https://doi.org/10.1109/TIE.2010.2066534>
- 4) Hu, X., Li, S., & Peng, H. (2012). A comparative study of equivalent circuit models for Li-ion batteries. *Journal of Power Sources*, 198, 359–367. <https://doi.org/10.1016/j.jpowsour.2011.10.013>
- 5) Kundur, P. (1994). *Power system stability and control*. McGraw-Hill.
- 6) MathWorks. (2024a). *quadprog—Quadratic programming*. MATLAB Optimization Toolbox Documentation. <https://www.mathworks.com/help/optim/ug/quadprog.html>
- 7) MathWorks. (2024b). *Quadratic programming algorithms*. MATLAB Optimization Toolbox Documentation. <https://www.mathworks.com/help/optim/ug/quadratic-programming-algorithms.html>
- 8) Omar, N., Daowd, M., Hegazy, O., Mulder, G., Timmermans, J. M., Coosemans, T., Van den Bossche, P., & Van Mierlo, J. (2014). Assessment of lithium-ion capacitor for use in hybrid electric vehicles and its battery aging. *Energies*, 7(4), 2015–2044. <https://doi.org/10.3390/en7042015>
- 9) Sauer, P. W., & Pai, M. A. (1998). *Power system dynamics and stability*. Prentice Hall.